

# OpenIBC: Open-Source Wake-Up Receiver for Capacitive Intra-Body Communication

Florian Wolling<sup>\*</sup>, Florian Hauck, Günter Schröder<sup>†</sup> & Kristof Van Laerhoven<sup>‡</sup>

University of Siegen, Department of Electrical Engineering and Computer Science, Siegen, Germany

<sup>\*</sup>florian.wolling@uni-siegen.de, <sup>†</sup>guenter.schroeder@uni-siegen.de, <sup>‡</sup>kvl@eti.uni-siegen.de

## Abstract

Intra-Body Communication (IBC) uses the human body as a part of the physical transmission channel for a more efficient and secure on-body communication. Since its introduction in 1995, it has evolved into an alternative to traditional wired and wireless techniques, and was eventually included as human body communication (HBC) in the IEEE 802.15.6 standard for wireless body area networks (WBAN). In contrast to the ubiquitous radio-frequency identification (RFID) and near-field communication (NFC), IBC has, however, not reached the market yet, and possible applications remain underinvestigated. We present the *OpenIBC* project and a first *open-source* IBC receiver that is based on a repurposed off-the-shelf low-power RFID wake-up receiver front-end. In the evaluation, the prototype achieved a data rate of 4096 bit/s with a packet error rate of  $320.0 \times 10^{-6}$  at a low power of  $7.4 \mu\text{W}$  in listening mode and  $8.4 \mu\text{W}$  when receiving data. The design files and software are made available to encourage researchers to replicate and improve on our work, and to explore potential applications that benefit from IBC.

## 1 Introduction and Motivation

Initiated by Zimmerman in 1995 [44], intra-body communication (IBC) evolved into a promising alternative for wireless body-area networks (WBAN). Somewhat located between the traditional wired and wireless techniques, it uses the confined human body as an efficient [8, 18] transmission medium to provide information physically secure [23] throughout the user’s skin. Large research teams regularly present new findings and fully integrated ASICs that continue to push the boundaries of what is possible. Nevertheless, none of the presented approaches ever reached the market, the implementations remained closed-source and are not turned into commercial products to make them available. With the discontinued attempt BodyCom [33], Microchip



**Figure 1.** The *OpenIBC* prototype with the proposed *open-source* IBC receiver, assembled from (left to right):  $30 \times 30 \text{ mm}^2$  electrodes with 1 cm air gap [41, 42], low-frequency OOK wake-up receiver ScioSense AS3930, 125 kHz LC band-pass filter with 7.2 mH inductance, TinyPICO NANO stamp module with ESP32 microcontroller, 3.7 V/60 mAh LiPo battery, and USB connector. Size of the assembled prototype:  $40 \times 67 \times 10 \text{ mm}^3$ .

provided the specialized analog front-end MCP2035 which, however, quickly disappeared while other companies seem to be cautious about investing. Due to the absence of commercially available IBC transceiver modules with low cost and complexity, research into potential applications is lagging behind. Especially concepts for more intuitive human-computer interaction (HCI) and their impact on the user experience (UX), therefore, cannot be explored yet.

We propose to repurpose off-the-shelf analog front-ends for RFID/NFC systems to implement *open-source* IBC interfaces which would enable a faster prototyping. In this paper, we present a first step toward this long-term goal. However, we do not intend to compete with cutting-edge research, especially not in terms of data rate and efficiency. Instead, we aim for the use of standard components to pave the way for applications that can directly be translated to future fully-integrated solutions, when finally made available.

Our main contributions are threefold:

- We motivate the *OpenIBC* project and take the first step toward an *open-source* intra-body communication transceiver from commercial off-the-shelf components.
- We present a wearable prototype based on the low-frequency OOK wake-up receiver ScioSense AS3930.
- We demonstrate the feasibility of repurposing an RFID front-end for IBC and evaluate the power consumption, wake-up latency, achievable data rate and packet errors.

## 2 Background

In 1995, Zimmerman et al. [44] presented a novel communication principle that is somewhat located between the traditional wired and wireless techniques while showing advantages over both. It uses the human body as a transmission medium to provide information throughout the user’s skin and was initially termed as intra-body communication (IBC). However, designated as human body communication (HBC), it is since 2012 included in the IEEE 802.15.6 standard [17] for wireless body area networks (WBAN), and is in research also referred to as body channel or body-coupled communication (BCC). The two primarily investigated IBC principles, surveyed in [22, 29], are the original capacitive coupling [44] and galvanic coupling [14, 21, 39]. Furthermore, reviewed in [37], unconventional approaches use electromagnetic fields [19, 31] and transdermal ultrasound [10], which has been subject of the previous EWSN workshop on “Intra-body embedded networks ...” in 2021 [11].

In this work, capacitive coupling is applied to modulate the electric field of the human body. With a typical magnitude of few pA, the induced displacement currents do not pose a health risk to the user [26, 37]. In contrast to the busy air channel, the body is still free and its limited distribution volume significantly improves the energy efficiency [8, 18]. At higher frequencies, however, the human body or parts of it act as a radiating antenna, hence narrowing the suitable frequency band to 100 kHz–50 MHz [1, 6, 18]. At these relatively low frequencies, the near field outside the confined body decays abruptly which makes IBC insusceptible to eavesdropping and physically secure [23]. The characterization and modeling of the body channel turned out to be difficult and findings vary widely depending on the setup and equipment used [22]. Primarily the measurement devices’ (unintended) grounding but also the port termination, typically to 50 Ω, have a large impact on the determined channel loss. The transmission behavior resembles a high-pass filter whose corner frequency lowers with increasing input impedance [22, 24]. Particularly at low frequencies, the body can be considered as a conductor to form the signal’s forward path with a marginal loss of about 0.5 dB [25]. The return path, however, is established via the environment, and the earth ground respectively, which has been identified to be the bottleneck of the channel circuit, resulting in a total channel loss of typically 45–55 dB [13, 30].

Research presented both experimental prototypes on a PCB level [12, 28, 41] as well as high-level, chip-casted ASICs [3, 5, 7, 23, 36] achieving a very high data rate of 80 Mbit/s at 8.9 mW [5] or even an outstanding efficiency of 1–20 kbit/s at 415 nW [23]. Nevertheless, none of the presented approaches ever reached the market, the implementations remained closed-source and are typically not turned into commercial products. Moreover, also the discontinued attempt BodyCom [33] with the specialized MCP2035 from Microchip quickly disappeared while other companies seem to be cautious about investing. Diverse commercial devices have been repurposed for IBC, applying fingerprint sensors and touchpads [15] as transmitters or touchscreens [16, 38] and ECG sensor front-ends [40] as receivers, unsurprisingly achieving only low data rates of 4–50 bit/s, however.

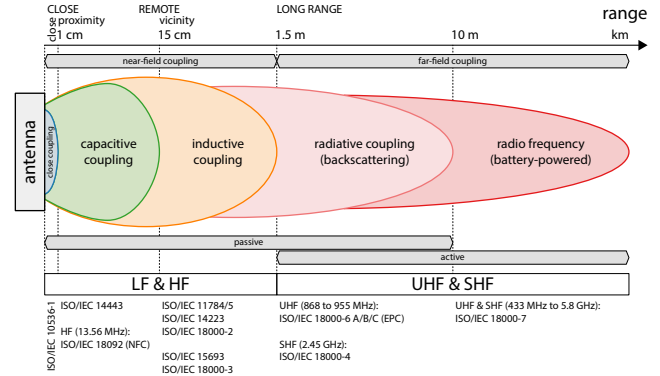


**Figure 2. Summary of the coupling principles, ranges, and typical ISO/IEC standards of RFID/NFC. cf. [35]**

In contrast, transceiver circuits for radio-frequency identification (RFID) and near-field communication (NFC) are fully developed and ubiquitous. Developed in the 1970/80s, the fundamental principle of RFID targets commercial low-cost applications which require the identification and tracking of tagged objects. A reader can obtain simple but unique information from a transponder tag in range, e.g. an identification number associated with the object. While active tags come along with their own energy source, enabling the response over larger distances in the far field, passive transponders take the required energy from the reader’s induction field and apply load modulation to provide a response in the near field. Most passive RFID transponders operate in the low frequency (LF, 125.0–134.2 kHz) and high frequency (HF, 13.56 MHz) bands which tend to be robust against interference. There are also passive tags using the ultra-high frequency (UHF, 433 MHz and 858–930 MHz) band, but UHF and super-high frequency (SHF, 2.4 or 5.8 GHz) microwaves are more common for active tags, enabling faster data transmission. Wrapped around the popular RFID standards, in 2002 Sony and Philips initiated the development of NFC for contactless, wireless communication between devices in close proximity (ISO/IEC 18092). Based on the 13.56 MHz HF band, it enables a bidirectional, peer-to-peer data transmission at high data rates of up to 424 kbit/s, but it is still downward compatible to passive targets. **Figure 2** summarizes the coupling principles, ranges, and standards. [9]

All of the aforementioned techniques suffer from receiver front-ends which often spend most of the energy for idle listening. Systems with rare or only sporadic, event-based communication, therefore, usually minimize their active time through a low duty cycle, at cost of higher latency, however. They regularly switch between sleep and receive mode, to listen to the channel and preferably not miss a message. Although the typical consumption of IBC transceivers is multiple orders lower than of conventional RF [24, 32], their dissipation is nevertheless predominant. Wake-up receivers are specifically designed for the continuous, always-on channel listening at low power. Usually, a long but low-frequency carrier burst is used to trigger a wake-up process that releases an interrupt request to activate the primary circuit, e.g. a microcontroller with more performance. For IBC, such systems have already been presented in [2, 4, 27, 32, 43].

### 3 Concept

In recent years, RFID and NFC turned into ubiquitous alternatives to traditional radio transmission for short- and medium-range communication. Instead of a dipole antenna for far-field radio propagation, usually a loop antenna is used for both data transmission and energy transfer via electromagnetic near-field coupling. Although capacitive coupling is being mentioned in the standard ISO/IEC 10536 for close coupling, its implementation, based on available front-ends, is not easily done by just replacing the coil with electrodes. Furthermore, the standard specifies a maximum range of 1 cm through air, which is not sufficient for typical WBANs. To overcome this hurdle, we propose to utilize the human body as an intermediate transmission medium. The desired evolution from conventional electromagnetic coupling via capacitive, electric field coupling toward capacitive intra-body coupling is illustrated in **Figure 3**. According to our concept, the transmitter induces signals via close coupling into the body and modulates its surrounding electric field. The receiver again couples to the body, detects the induced fluctuations in the electric field, and demodulates the desired signal. While the forward path is established via the human tissue, which at the targeted frequencies virtually acts like a conductor [25], the return path, to close the channel circuit, is formed through the environment, the earth ground respectively [13, 30]. We thus conclude that, in principle, it should be possible to repurpose RFID/NFC transceivers for IBC.

Unfortunately, the use of these analog front-ends comes along with multiple obstacles due to fundamental differences of RFID/NFC compared to the IBC principle. Several integrated circuits are available which enable the implementation of tags or wireless sensors. The majority acts, however, as a passive transponder/target, supplied by an active reader/initiator via electromagnetic induction, and the requested information are returned through load modulation.

The current density of the signal, induced at the excitation electrode on the skin, has to conform with safety regulations such as the standard of the international commission on non-ionizing radiation protection (ICNIRP) [20]. Therefore, the maximum amount of energy that can be transferred through the human tissue is limited. The typical displacement current induced is, however, multiple orders smaller than the allowed maximum [26, 37]. Although demonstrated in [34], the remote supply of devices and the use of backscattering or even load modulation are, therefore, at least difficult. Instead, the active signal generation and a more advanced peer-to-peer connection are required, similar to NFC. The popular, fully integrated multi-protocol RFID/NFC transceiver TRF7970A from Texas Instruments<sup>1</sup> supports all desirable standards. It is, nevertheless, optimized for inductive coupling and hence shows not only a low output impedance of 4 or 8  $\Omega$ , but also a relatively low input impedance of 10 k $\Omega$ . In preliminary experiments, impedance matching to this circuit, from high to low  $Z$ , turned out to be cumbersome. Continued research revealed the AS3930 from ScioSense, which shows promising characteristics such as a high input impedance.

<sup>1</sup>TRF7970A, Texas Instruments:  
<https://www.ti.com/product/TRF7970A> (date accessed: 2022-05-12).

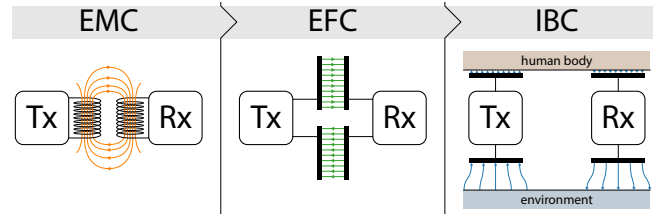


**Figure 3. Evolution from conventional electromagnetic, inductive near-field coupling (EMC) via uncommon electric field, capacitive coupling (EFC) toward intra-body coupling/communication (IBC) which utilizes the human body to extend the capacitive close-coupling range.**

### 4 System Design

As a first step toward an *open-source* IBC transceiver, we present a receiver circuit based on the low-power wake-up receiver front-end AS3930 from ScioSense. It is originally designed for reading active RFID tags in applications such as operator identification, access control, object localization, or wireless sensing. The proposed system consists of the wake-up receiver IC itself, two coupling electrodes, an adjoined LC filter circuit, and an ESP32 microcontroller to be woken up on data reception. Embedded into a suitable channel model, the circuit is simulated to estimate its performance. The considerations made are detailed in the following.

**Frequency Band:** Essential requirement is the use of a free and unlicensed frequency spectrum. The LF and HF bands, typically applied in RFID and NFC systems, are located in the ISM band, internationally reserved for industrial, scientific, and medical purposes. Given by the selected IC, the 125 kHz LF band is applied. It shows good resistance to interference but the long wavelength requires larger components compared to those applied for the 13.56 MHz HF band.

**Receiver:** The AS3930 from ScioSense<sup>2</sup> is a low-power OOK wake-up receiver for LF signals. With a 110–150 kHz bandwidth, its input is optimized for a 125 kHz carrier frequency  $f_0$ , at which it shows a comparatively high input impedance of 2 M $\Omega$ . It is designed to continuously run as an always-on wake-up receiver that allows to activate a connected system on detection of a carrier burst with a sensitivity of 100  $\mu\text{V}_{\text{RMS}}$ . After the successful correlation of a custom signal pattern, the following data is demodulated and streamed to the microcontroller which puts the front-end back to listening mode when reception is complete. The chip can be supplied with 2.4–3.6 V and draws, according to the datasheet, 2.7  $\mu\text{A}$  in continuous listening mode and 5.3  $\mu\text{A}$  when correlating the wake-up pattern or receiving data.

**Microcontroller:** The receiver IC does not provide computing power for applications itself. It is only intended to wake up a connected circuit via interrupt request and to then forward the demodulated, received data. The selection of a suitable microcontroller depends on the target application. To allow for an easy setup and to provide sufficient performance for evaluation purposes, we decided for the popular ESP32 from Espressif Systems in form of a small TinyPICO

<sup>2</sup>AS3930, ScioSense:  
<https://www.sciosense.com/products/wireless-sensor-nodes/as3930-lf-receiver-ic/> (date accessed: 2022-05-12).

NANO<sup>3</sup> stamp module. The powerful SoC provides diverse operation modes, in particular a deep sleep mode at less than 20  $\mu\text{A}$  that enables battery-powered applications.

**Transmitter:** Since this paper concentrates on the receiver front-end, the transmitter is kept simple and is based on the same stacked electrode setup as the receiver. Instead of using a power amplifier to boost the amplitude [44], the signal is directly modulated with an ESP32 microcontroller which regularly (e.g. every 10 ms) generates a wake-up signal with a 3.3  $V_{\text{pp}}$  amplitude, 1.17  $V_{\text{RMS}}$  respectively. As detailed below, the transmitter is grounded through the mains' neutral wire, which considerably reduces the channel loss.

**Protocol:** The AS3930 supports two wake-up protocols. While the first one consists of a burst directly followed by the data, the second one adds a preamble for clock recovery and a programmable 16bit wake-up pattern for a more reliable detection of the desired signal through correlation. The data is preferably Manchester encoded, which results in eight applicable symbol rates ranging from 512–4096 S/s with a period time per symbol and bit  $t_{\text{bit}}$  of 1.953–0.244 ms. Applying the advanced protocol requires first a long carrier burst of  $0.360 \text{ ms} < t_{\text{burst}} < 16 \times t_{\text{bit}}$  (e.g. 1 ms), followed by a preamble of  $t_{\text{pre}} > 4 \times t_{\text{bit}}$ , and a wake-up pattern of  $t_{\text{pat}}$ , considering that  $t_{\text{pre}} + t_{\text{pat}} < 40 \times t_{\text{bit}}$ , before the desired data (e.g. 2 byte,  $16 \times t_{\text{bit}}$ ) is sent. While lower data rates are more immune to ambient noise, higher rates require a wider bandwidth to also pass sidebands through for a faster transient response. This results in a more accentuated envelope but also injects a larger portion of the noise.

**Electrode Setup:** A setup of two  $30 \times 30 \text{ mm}^2$  electrodes with an air gap of 1 cm is used which has previously been applied and characterized in [41, 42]. The design reduces the dielectric material between the electrodes, minimizes the intrinsic capacitance, and hence maximizes the coupling through the tissue. The use of the LF band, and hence the modulation of the quasi-electrostatic field, is “eliminating the necessity for high-frequency design and complex hardware components” [12]. The ideal intrinsic capacitance  $C_{\text{int}}$  of the formed parallel plate capacitor is 0.797 pF:

$$C = \epsilon_0 \epsilon_r \frac{A}{d} \quad (1)$$

Worn at the wrist during diverse activities, measurements with an AD7151<sup>4</sup> capacitance-to-digital converter (CDC) have shown that the electrodes'  $C_{\text{rx}}$ , including parasitic effects, typically fluctuates around  $0.987 \pm 0.234 \text{ pF}$  [42].

**LC Band-Pass Filter:** The AS3930 requires an external band-pass filter to extract the desired signal at  $f_0$  of 125 kHz. Implemented as a rejector in parallel to the input circuit, with a high but limited impedance of  $2 \text{ M}\Omega$ , it drains undesired components outside the intended frequency band, e.g. ambient noise. The filter is implemented as a parallel LC resonant circuit whose resonant frequency  $f_r$  with  $\omega = 2\pi f$  is:

$$\omega_r = \frac{1}{\sqrt{LC}} \quad (2)$$

<sup>3</sup>TinyPICO NANO, Unexpected Maker:

<https://www.tinypico.com/tinypico-nano> (date accessed: 2022-05-12).

<sup>4</sup>AD7151, Analog Devices:

<https://www.analog.com/en/products/ad7151.html> (date accessed: 2022-05-12).

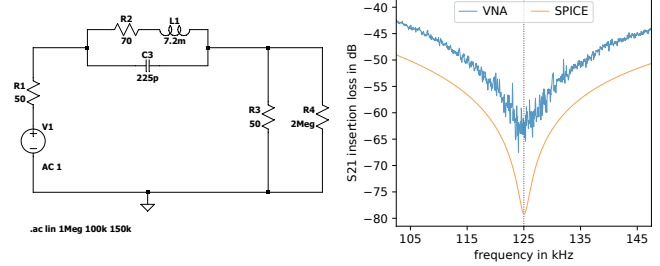


**Figure 4.** SPICE model of the LC resonant circuit between the ports 1 and 2 of the VNA (left). Simulation and measurement of the S21 insertion loss for 125 kHz (right).

Given the complex impedances  $Z_L = j\omega L$  and  $Z_C = \frac{1}{j\omega C}$ , the ideal impedance  $Z_{LC} = Z_L || Z_C$  maximizes at  $\omega_r$ :

$$\lim_{\omega \rightarrow \omega_r} Z_{LC}(\omega) = \infty \quad (3)$$

In RFID/NFC applications, the filter normally consists of the coupling coil with a specific inductance and a countering capacitor to form the resonant tank circuit. In the intended IBC receiver, however, only the inductance  $L$  is fixed while the capacitance  $C$  is given through the inter-electrode capacitance  $C_{\text{rx}}$  and hence fluctuating as mentioned before. It is composed of  $C_{\text{int}}$  and the parasitic coupling through body and environment, which is essential for IBC. Consequently,  $f_r$  deviates from  $f_0$  and shifts slightly according to the affected  $C_{\text{rx}}$ . The selection of real, discrete components appeared to be difficult. The  $C_{\text{rx}}$  with around 1 pF is too small and, in combination with the low  $f_r$ , it would require a huge  $L$  of 1.6 H, meaning many windings and thus large dimensions. With the transponder coil B82450A7204A from TDK<sup>5</sup> we found a suitable component that is available at a maximum of 7.2 mH, and its size of  $11.4 \times 3.5 \times 2.4 \text{ mm}^3$  also meets the spatial requirements. To nevertheless reach the resonant state, according to (2),  $C_{\text{rx}}$  is enhanced with  $C_{\text{add}}$  of 224 pF to reach the required 225.16 pF. **Figure 4** shows the circuit's SPICE simulation and S21 parameter characterization.

**Channel Model:** For LF IBC systems ( $f_0 < 1 \text{ MHz}$ ) in the quasi-electrostatic domain, and with a capacitive high-impedance termination at the receiver, the channel model of [24] is valid. The applied lumped SPICE model is illustrated in **Figure 5**. Accordingly, the channel loss largely depends on the capacitances that form between the environment and the transmitter  $C_{\text{ret,tx}}$ , the receiver  $C_{\text{ret,rx}}$ , the body  $C_{\text{body}}$ , and the load at the receiver side  $C_{\text{load}}$ , approximated by [24]:

$$\text{loss}_{\text{dB}} \approx 20 \log_{10} \left( \frac{C_{\text{body}} \cdot C_{\text{load}}}{C_{\text{ret,tx}} \cdot C_{\text{ret,rx}}} \right) \quad (4)$$

While larger  $C_{\text{ret,tx}}$  and  $C_{\text{ret,rx}}$  in the return path reduce the channel loss, larger  $C_{\text{body}}$  and  $C_{\text{load}}$  increase it. Due to the imbalance  $1:224$  of  $C_{\text{rx}}$  and  $C_{\text{add}}$ , fluctuations of  $C_{\text{rx}}$  do not considerably affect  $f_r$ . The extended  $C_{\text{load}} = C_{\text{rx}} + C_{\text{add}}$  is, however, not ideal as it limits the receiver's efficiency and sensitivity. To compensate for this effect, the transmitter is con-

<sup>5</sup>B82450A7204A, TDK:

<https://www.tdk-electronics.tdk.com/inf/30/db/ind.2008/b82450a.a.pdf> (date accessed: 2022-05-12).

nected to ground. The simulation allows to estimate whether the signal would reach the required sensitivity threshold of  $100\ \mu\text{V}_{\text{RMS}}$ . In line with the conducted experiments, the use of a grounded transmitter is required to enable the successful signal transmission to a floating receiver device.

## 5 Evaluation

The prototype is evaluated regarding power consumption, wake-up latency, achievable data rate, and packet error rate.

**Power Consumption:** The Power Profiler Kit II from Nordic Semiconductor<sup>6</sup> is used to precisely monitor the consumed power. Excerpts are provided in Figure 6. The ESP32 microcontroller is not considered part of the receiver and does not count toward the determined values. The used front-end allows for a very low average power of  $7.4\ \mu\text{W}$  ( $2.24\ \mu\text{A}$  at  $3.3\ \text{V}$ ) in listening mode and of  $8.4\ \mu\text{W}$  ( $2.56\ \mu\text{A}$  at  $3.3\ \text{V}$ ) during the reception of a wake-up signal and the data.

**Wake-Up Latency:** The wake-up latency describes the delay between the initiation of the wake-up signal at the transmitter and its successful detection at the receiver, excluding the data transmission itself. As an example, it sums up from a burst of  $1000\ \mu\text{s}$ , a preamble of  $1220\ \mu\text{s}$  ( $5 \times t_{\text{bit}}$ ), and the pattern of  $1952\ \mu\text{s}$  ( $8 \times t_{\text{bit}}$ ) to a total of  $4172\ \mu\text{s}$ . To measure the latency, an output pin of the transmitter is directly wired to an input pin of the receiver, enabling the notification of an initiated transmission. The receiver then determines the time passed between the detection of the flag and the interrupt request from the receiver circuit. For 100000 packets, the latency showed to be stable with  $4215 \pm 3.6\ \mu\text{s}$ .

**Data and Error Rate:** The achievable data rate primarily depends on the packet error rate (PER) which is the ratio of erroneous packets and number of packets sent. High data rates require shorter symbols and hence a wider filter bandwidth for a faster transient response of the signal envelope. In this way, more ambient noise is injected which results in more symbol errors. Lower data rates are, therefore, more robust because larger symbols are transmitted which are less affected by less noise. A single subject (male, 29) wore the prototype at one wrist while touching the transmitter's electrode with the palm of the other hand. The arms were kept wide apart and away from objects which would improve the direct coupling between the electrodes. On three days with different weather conditions, the transmitter sent 100000 wake-up sequences at a rate of 100 Hz, each time taking 16.7 min. At the maximum data rate of 4096 bit/s, with a wide passband but lower sensitivity ( $27\ \text{k}\Omega$  shunt resistor enabled), the achieved average PER is  $320.0 \times 10^{-6}$ .

**Limitations:** Although the analog front-end AS3930 is quite sensitive ( $100\ \mu\text{V}_{\text{RMS}}$ ), the presented prototype does not enable fully wearable systems yet. While the receiver can be worn floating, at least the transmitter is still required to be grounded, to reduce the channel loss by about 40–45 dB. Moreover, the applied 125 kHz LF band is located at the lower bound of the applicable IBC spectrum [1, 6, 18]. The use of the 13.56 MHz HF band instead would not only reduce component size but also increase the potentially achievable

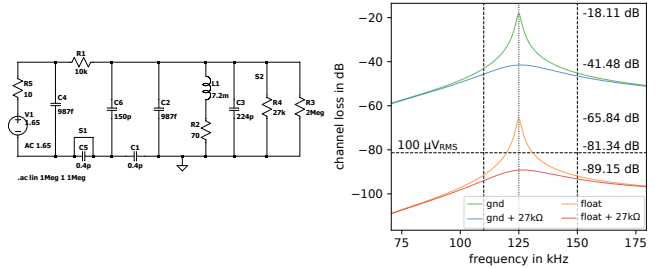


**Figure 5. Lumped circuit, SPICE model for the simulation of the LF, high-impedance IBC receiver front-end, according to [24]. S1: floating or grounded transmitter; S2: dis-/enabled shunt resistor of  $27\ \text{k}\Omega$  for a wider filter bandwidth but lower sensitivity. Simulation (right): front-end's bandwidth (verticals), sensitivity threshold at  $100\ \mu\text{V}_{\text{RMS}}$  (horizontal), grounded (gnd) and floating (float) transmitter, dis-/enabled shunt resistor ( $27\ \text{k}\Omega$ ).**

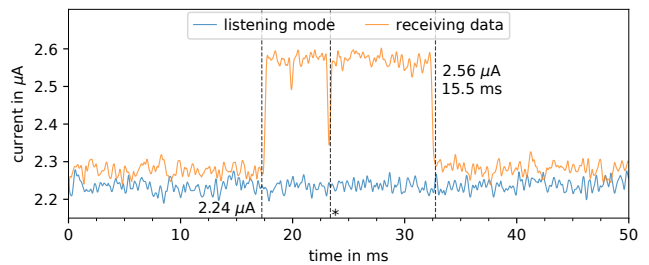


**Figure 6. Excerpts from the current measurements with the Power Profiler Kit II from Nordic Semiconductor. Consumption in listening mode (blue) and during data reception (orange), after a successful pattern correlation (\*). Sampled at 100 kHz and denoised using a  $2 \times 2^{\text{nd}}$  order zero-phase 2.5 kHz low-pass Butterworth IIR filter.**

data rate to NFC levels, toward a maximum of 424 kbit/s. It might also eliminate the need to expand  $C_{\text{rx}}$  by  $C_{\text{add}}$  for resonance, diminish  $C_{\text{load}}$ , and hence reduce the channel loss.

## 6 Conclusions

IBC is an unconventional but promising communication principle that has not reached the market yet. In this paper, we presented an *open-source* IBC receiver based on the commercially available AS3930 wake-up receiver front-end, originally designed for reading active RFID tags. Its high input impedance enables the capacitive signal reception in the 125 kHz low frequency band with up to 4096 bit/s and a packet error rate of  $320.0 \times 10^{-6}$ . The designed, simulated, and evaluated prototype draws a low power of  $7.4\ \mu\text{W}$  when listening to the channel and  $8.4\ \mu\text{W}$  during data reception. The sensitivity of  $100\ \mu\text{V}_{\text{RMS}}$  is not sufficient for the intended use in fully wearable applications yet. Therefore, the next step is to develop a pre-amplifying circuit which would further improve the front-end's input impedance, lower the load capacitance, and in turn improve the sensitivity.

With *OpenIBC*, we encourage researchers to replicate and improve on our work, to develop *open-source* IBC transceivers and to explore their potential applications. The design files and software of the prototype are made available for download in our public GitHub repository:

<https://github.com/fwolling/OpenIBC/>

<sup>6</sup>Power Profiler Kit II, Nordic Semiconductor: <https://www.nordicsemi.com/Products/Development-hardware/Power-Profiler-Kit-2> (date accessed: 2022-05-12).

## 7 References

- [1] J. Bae, H. Cho, K. Song, H. Lee, and H.-J. Yoo. The signal transmission mechanism on the surface of human body for body channel communication. *IEEE TMITT*, 60(3):582–593, 2012.
- [2] J. Bae and H.-J. Yoo. A 45  $\mu\text{w}$  injection-locked fsk wake-up receiver with frequency-to-envelope conversion for crystal-less wireless body area network. *IEEE JSSC*, 50(6):1351–1360, 2015.
- [3] B. Chatterjee, A. Datta, M. Nath, G. K. K. N. Modak, and S. Sen. A 65nm 63.3 $\mu\text{w}$  15mbps transceiver with switched-capacitor adiabatic signaling and combinatorial-pulse-position modulation for body-worn video-sensing ar nodes. In *IEEE ISSCC*, pages 276–278. IEEE, 2022.
- [4] H. Cho, J. Bae, and H.-J. Yoo. A 37.5  $\mu\text{w}$  body channel communication wake-up receiver with injection-locking ring oscillator for wireless body area network. *IEEE TCSI*, 60(5):1200–1208, 2013.
- [5] H. Cho, H. Kim, M. Kim, J. Jang, Y. Lee, K. J. Lee, J. Bae, and H.-J. Yoo. A 79 pJ/b 80 mb/s full-duplex transceiver and a 100 kb/s super-regenerative transceiver for body channel communication. *IEEE JSSC*, 51(1):310–317, 2016.
- [6] N. Cho, L. Yan, J. Bae, and H.-J. Yoo. A 60 kb/s–10 mb/s adaptive frequency hopping transceiver for interference-resilient body channel communication. *IEEE JSSC*, 44(3):708–717, 2009.
- [7] C.-C. Chung, C.-T. Chang, and C.-Y. Lin. A 1 mb/s–40 mb/s human body channel communication transceiver. In *VLSI-DAT*, pages 1–4. IEEE, 2015.
- [8] J. H. Donker. The body as a communication medium. In *Department of EMCS, 11th Conference on IT, University of Twente*, 2009.
- [9] K. Finkenzeller. *RFID Handbook: Fundamentals and Applications in Contactless Smart Cards, Radio Frequency Identification and Near-Field Communication*. Wiley and IEEE Press, 3rd edition, 2010.
- [10] L. Galluccio, T. Melodia, S. Palazzo, and G. E. Santagati. Challenges and implications of using ultrasonic communications in intra-body area networks. In *WONS*, pages 182–189. IEEE, 2012.
- [11] L. Galluccio, A. Vizziello, and P. Savazzi. Intra-body embedded networks exploiting ultrasounds and coupling technologies, 2021. EWSN workshop.
- [12] T. Große-Puppenthal, S. Herber, et al. Capacitive near-field communication for ubiquitous interaction and perception. In *UbiComp '14*, pages 231–242. ACM, 2014.
- [13] T. Große-Puppenthal, C. Holz, G. Cohn, R. Wimmer, O. Bechtold, S. Hodges, M. S. Reynolds, and J. R. Smith. Finding common ground: A survey of capacitive sensing in human-computer interaction. *CHI '17*, page 3293–3315. ACM, 2017.
- [14] T. Handa, S. Shoji, S. Ike, S. Takeda, and T. Sekiguchi. A very low-power consumption wireless eeg monitoring system using body as a signal transmission medium. In *Transducers 97*, pages 1003–1006. IEEE, 1997.
- [15] M. Hesar, V. Iyer, and S. Gollakota. Enabling on-body transmissions with commodity devices. In *UbiComp*, page 1100–1111. ACM, 2016.
- [16] C. Holz and M. Knaust. Biometric touch sensing: Seamlessly augmenting each touch with continuous authentication. In *UIST'15*, pages 303–312, New York, 2015. ACM.
- [17] IEEE Standards Association. IEEE 802.15.6-2012 - Wireless Body Area Networks, 2012.
- [18] B. Kibret, A. K. Teshome, and D. T. H. Lai. Human body as antenna and its effect on human body communications. *Progress In Electromagnetics Research (PIER)*, 148:193–207, 2014.
- [19] F. Koshiji, N. Yuyama, and K. Koshiji. Wireless body area communication using electromagnetic resonance coupling. In *CPMT Symposium Japan*, pages 1–4. IEEE, 2012.
- [20] J. Lin, R. Saunders, K. Schulmeister, P. Söderberg, A. Swerdlow, M. Taki, B. Veyret, G. Ziegelberger, M. H. Repacholi, R. Matthes, A. Ahlbom, K. Jokela, and C. Roy. ICNIRP guidelines for limiting exposure to time-varying electric and magnetic fields (1 hz to 100 khz). *Health Physics*, 99:818–836, 2010.
- [21] D. P. Lindsey, E. L. McKee, M. L. Hull, and S. M. Howell. A new technique for transmission of signals from implantable transducers. *IEEE TBME*, 45(5):614–619, 1998.
- [22] S. Maity, D. Das, B. Chatterjee, and S. Sen. Characterization and classification of human body channel as a function of excitation and termination modalities. In *IEEE EMBC*, pages 3754–3757, 2018.
- [23] S. Maity, N. Modak, D. Yang, S. Avlani, M. Nath, J. Danial, D. Das, P. Mehrotra, and S. Sen. A 415 nw physically and mathematically secure electro-quasistatic hbc node in 65nm cmos for authentication and medical applications. In *CICC*, pages 1–4. IEEE, 2020.
- [24] S. Maity, N. Modak, D. Yang, M. Nath, S. Avlani, D. Das, J. Danial, P. Mehrotra, and S. Sen. Sub- $\mu\text{w}$ comm: 415-nw 1–10-kb/s physically and mathematically secure electro-quasi-static hbc node for authentication and medical applications. *IEEE JSSC*, 56(3):788–802, 2021.
- [25] S. Maity, K. Mojabe, and S. Sen. Characterization of human body forward path loss and variability effects in voltage-mode hbc. *IEEE LMWC*, 28(3):266–268, 2018.
- [26] S. Maity, M. Nath, G. Bhattacharya, B. Chatterjee, and S. Sen. On the safety of human body communication. *IEEE TBME*, 67(12):3392–3402, 2020.
- [27] S. Maity, D. Yang, B. Chatterjee, and S. Sen. A sub-nw wake-up receiver for human body communication. In *BioCAS*, pages 1–4. IEEE, 2019.
- [28] M. Moralis-Pegios, P. Alexandridou, and C. Koukourlis. Applying pulse width modulation in body coupled communication. *Journal of Electrical and Computer Engineering*, 2015:1–6, 2015.
- [29] D. Naranjo-Hernández, A. Callejón-Leblic, et al. Past results, present trends, and future challenges in intrabody communication. *Wireless Communications and Mobile Computing*, 2018:1–39, 2018.
- [30] M. Nath, S. Maity, and S. Sen. Toward understanding the return path capacitance in capacitive human body communication. *IEEE TCSI*, 67(10):1879–1883, 2020.
- [31] J. Park and P. P. Mercier. Magnetic human body communication. *IEEE EMBC*, 2015:1841–1844, 2015.
- [32] J. Petäjäjärvi, K. Mikhaylov, R. Vuontoniemi, H. Karvonen, and J. Iinatti. On the human body communications: wake-up receiver design and channel characterization. *EURASIP Journal on Wireless Communications and Networking*, 2016(1):1–17, 2016.
- [33] C. Pop. AN1391: Introduction to the bodycom technology. *Microchip Technology Inc.*, 2011.
- [34] E. R. Post, M. Reynolds, M. Gray, J. Paradiso, and N. Gershenfeld. Intrabody buses for data and power. In *ISWC*, pages 52–55. IEEE, 1997.
- [35] K. Sattlegger and U. Denk. Navigating your way through the rfid jungle. *White Paper, Texas Instruments*, 2014.
- [36] S.-J. e. a. Song. A 0.2-mw 2-mb/s digital transceiver based on wide-band signaling for human body communications. *IEEE Journal of Solid-State Circuits*, 42(9):2021–2033, 2007.
- [37] W. J. Tomlinson, S. Banou, C. Yu, M. Stojanovic, and K. R. Chowdhury. Comprehensive survey of galvanic coupling and alternative intra-body communication technologies. *IEEE Communications Surveys & Tutorials*, 21(2):1145–1164, 2019.
- [38] T. Vu, A. Baid, S. Gao, M. Gruteser, R. Howard, J. Lindqvist, P. Spasojevic, and J. Walling. Distinguishing users with capacitive touch communication. In *MobiCom*, page 197–208. ACM, 2012.
- [39] M. S. Wegmueller, A. Kuhn, J. Froehlich, M. Oberle, N. Felber, N. Kuster, and W. Fichtner. An attempt to model the human body as a communication channel. *IEEE TBME*, 54(10):1851–1857, 2007.
- [40] F. Wolling, C. D. Huynh, and K. van Laerhoven. IBSync: Intra-body synchronization of wearable devices using artificial eeg landmarks. In *ISWC*, pages 102–107. ACM, 2021.
- [41] F. Wolling, P. M. Scholl, et al. Combining capacitive coupling with conductive clothes: Towards resource-efficient wearable communication. In *ISWC*, page 146–149. ACM, 2017.
- [42] F. Wolling, K. van Laerhoven, J. Bilal, P. M. Scholl, and B. Volker. WetTouch: Touching ground in the wearable detection of hand-washing using capacitive sensing. In *PerCom Workshops*, pages 769–774. IEEE, 2022.
- [43] L. Yongsu and Y. Hoi-Jun. A 274 $\mu\text{w}$  clock synchronized wireless body area network ic with super-regenerative rssi for biomedical ad-hoc network system. *IEEE EMBC*, 2017:710–713, 2017.
- [44] T. G. Zimmerman. Personal area networks: Near-field intra-body communication. *IBM systems Journal*, 35(3.4):609–617, 1996.